Systematic studies on effects of cationic ordering on structural and magnetic properties in Sr_2FeMoO_6

Y. H. Huang,[1,2,*] M. Karppinen,[1] H. Yamauchi,[1] and J. B. Goodenough[2]
[1]*Materials and Structures Laboratory, Tokyo Institute of Technology, Yokohama 226-8503, Japan*
[2]*Texas Materials Institute, ETC 9.102, The University of Texas at Austin, Austin, Texas 78712, USA*
(Received 4 September 2005; revised manuscript received 23 November 2005; published 9 March 2006)

Sr_2FeMoO_6 samples with various degrees of Fe, Mo ordering were prepared from a sol-gel-derived precursor with a sample-encapsulation technique. The order parameter ξ for Fe and Mo, determined by Rietveld refinement, ranged from 0.56 to 0.95. Structural data suggest that the equilibration reaction $Fe^{III}+Mo^{V}=Fe^{II}+Mo^{VI}$ is shifted toward the left by the trapping of minority-spin electrons in Mo-rich trap states for $\xi<0.7$ and that it is shifted toward the right at a transition from polaronic to itinerant minority-spin electrons at $\xi\approx 0.9$. In accord with a first-order polaronic-itinerant electronic transition, well-ordered itinerant-electron regions appear to be nucleated and to grow in a partially ordered matrix until they meet at antiphase boundaries. This heterogeneous development is at odds with models of homogeneous site disorder with a constant oxidation state of the Fe and Mo atoms.

DOI: 10.1103/PhysRevB.73.104408 PACS number(s): 75.30.Cr, 75.30.Mb, 72.80.Ng, 64.60.Cn

I. INTRODUCTION

The double-perovskite Sr_2FeMoO_6 has attracted considerable interest as a room-temperature, half-metallic ferromagnet for spintronic applications.[1] In the ideal double-perovskite structure, $FeO_{6/2}$ octahedra share corners with six $MoO_{6/2}$ octahedra, and *vice versa*. It has long been recognized that, given a periodic potential, a majority-spin $3d^5$ configuration may be localized in the presence of itinerant minority-spin electrons on the same atom in a *d* band containing only one electron.[2] In ideally ordered Sr_2FeMoO_6, the Mo^{VI}/Mo^{V} redox couple overlaps in energy, the Fe^{III}/Fe^{II} redox couple, so the minority-spin electrons are shared between the Fe and Mo atoms in an itinerant-electron π^* band. These minority-spin electrons are half-metallic, being of only one spin, and they couple the localized $S=5/2$ spins on the Fe atoms ferromagnetically.[3,4] However, ideal order is rarely, if ever, achieved in Sr_2FeMoO_6 because order is nucleated at different places in the crystal. These ideally ordered regions may be out of phase and therefore meet at an antiphase boundary containing $(180°-\phi)$ Fe-O-Fe or Mo-O-Mo interactions rather than Fe-O-Mo interactions. The Fe-O-Fe interactions are antiferromagnetic and couple the magnetizations of neighboring well-ordered ferromagnetic regions antiparallel at low applied fields to give a *B-H* hysteresis loop with negligible remanence and coercivity.[5] The Mo-O-Mo interactions may trap two electrons in a molecular orbital. Although the magnetization may saturate in a field as low as 2 kOe because of the large torque exerted on the ferromagnetic regions and the relatively small number of antiferromagnetic interactions across the antiphase boundary, nevertheless the saturation magnetization at 4 K remains below the theoretical $4\mu_B$/fu because of the existence of 360° domain walls at the antiphase boundaries.

Where there is incomplete site ordering within the ordered domains, the problem becomes more complex since perturbation of the periodic electron potential may destroy the itinerant character of the minority-spin electrons. In addition, electrons may be trapped in Mo-rich clusters within a partially ordered region. Spin-paired, trapped electrons would not contribute to the effective paramagnetic moment μ_{eff} attained from a Curie-Weiss law. Moreover, antiferromagnetic interactions between ferromagnetic, well-ordered regions has been shown[5] to give a Curie-Weiss law with Curie and Weiss constants that vary with the applied magnetic-field strength. These complications are manifest in reported μ_{eff} values that vary from 4.2 to $6.7\mu_B$/fu.[6–9] Consequently, attempts like that of Ogale *et al.*[10] to model the effects of site disorder on the magnetization without taking account of either spin pairing in Mo-rich traps, segregation into ordered and partially ordered regions, or the antiphase boundaries are suspect. In this paper, we have deliberately introduced site disorder into the ordered regions and investigated systematically the effects of this disorder on the structural, magnetic, and transport properties.

II. EXPERIMENTAL

Sr_2FeMoO_6 samples were synthesized by an encapsulation technique using a precursor obtained by a wet chemical route based on the thermal decomposition of metal complexes, as described in detail in a previous paper.[9] Stoichiometric $SrCO_3$, $Fe(NO_3)_3\cdot 9H_2O$ and $(NH_4)_6Mo_7O_{24}\cdot 4H_2O$ were used as starting materials, and ethylenediaminetetraacetic acid (EDTA) as a complexant. The precursor was calcined in air at 900 °C for 15 h before being pelletized, encapsulated into an evacuated, fused-quartz ampoule containing Fe grains to act as a getter for oxygen;[11] the samples were finally sintered at 900 °C–1150 °C for 24–100 h to achieve a Sr_2FeMoO_6 sample series with different Fe-Mo ordering.

The phase purity was checked by x-ray powder diffraction (XRD; Rigaku: RINT-2000 equipped with a rotating copper anode; Cu K_α radiation). The diffraction profiles were further analyzed with a Rietveld refinement program, RIETAN 2000,[12] to obtain the lattice parameters, atomic positions, and

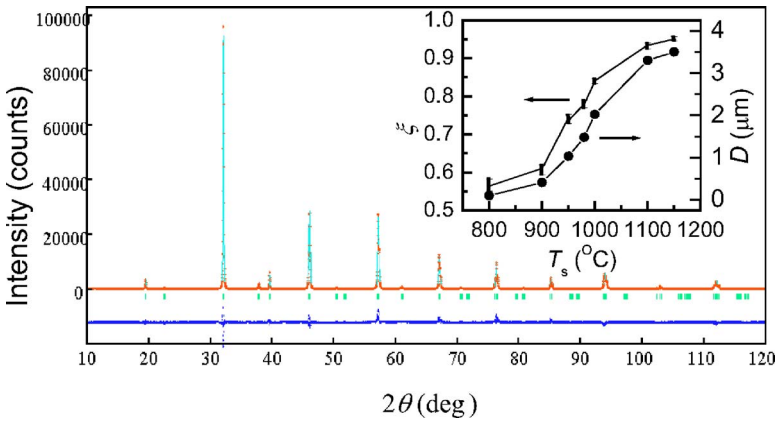

FIG. 1. (Color online) Experimental (solid lines) and calculated by Rietveld refinement (crosses) XRD patterns for a Sr_2FeMoO_6 sample sintered at 1150 °C for 100 h. Differences between the experimental and calculated intensity are shown in the bottom, and the small bars indicate the angular positions of the allowed Bragg reflection. The inset shows the evolution with sintering temperature T_s of the order parameter ξ and the average grain size D estimated by SEM images.

site-specific occupancies. Micrographs of the samples were taken with a scanning electron microscope (SEM; Hitachi: S4500). Magnetization measurements were made with a superconducting quantum interference device (SQUID; Quantum Design: MPMS-XL5). Resistance was measured with a standard four-probe technique and a commercial apparatus (PPMS; Quantum Design: System-Model 6000).

III. RESULTS AND DISCUSSION

In order to gain insight into the real effects of the site disorder, it is very important to obtain Sr_2FeMoO_6 samples of high quality. In our previous paper,[9] we demonstrated that the encapsulation technique with the sol-gel-derived product as a precursor and the Fe/FeO redox couple as an oxygen getter was an efficient route to prepare pure Sr_2FeMoO_6 with controllable site disorder. With this encapsulation technique, all the synthesized Sr_2FeMoO_6 samples in the present work were phase pure by judging from the XRD data, and their diffractions patterns were well refined in the tetragonal space group $I4/m$.[13,14] As shown in our previous paper,[9] we examined the purity carefully and proved that the content of any metallic Fe impurity that is invisible via x-ray diffraction or Mössbauer spectroscopy was less than 0.1 wt% in a typical sample. This examination was made by measurement of the field-dependent susceptibility above the Curie temperature T_C, i.e., by the same method used in Ref. 6. In addition, with the XRD intensities on a logarithmic scale, no $SrMoO_4$ impurity was detected. Since $SrMoO_4$ is nonmagnetic, even a small amount of it that cannot be visible by XRD has little influence on the magnetic properties.

Figure 1 displays experimental and calculated room-temperature diffraction profiles for a sample sintered at 1150 °C for 100 h. The lattice parameters for the sample were determined as $a=5.5754(1)$ Å and $c=7.9052(1)$ Å; the value of the order parameter ξ, calculated as $\xi=2(g_{Fe}-0.5)$ from the refined occupancy of Fe at its correct site (g_{Fe}), was found as high as 0.95. For the sample series synthesized for the present study, ξ ranges from 0.56 to 0.95. As seen in our previous paper,[9] SEM images show a highly homogeneous morphology with well-defined regular grains. Thus, the average grain size D can be estimated from SEM images by directly measuring the diameters of the separate grains. It is found that both D and ξ strongly depend on the sintering temperature T_s. The inset of Fig. 1 shows the values of D and ξ for the samples sintered at various T_s for 50 h. The dependences of D and ξ on T_s are essentially parallel, indicating that a less-ordered sample has a smaller D value. For example, D ranges from ~100 nm to ~3.8 μm for the samples with $\xi=0.56$ to 0.95.

In Fig. 2, lattice parameters and the unit-cell volume are plotted against ξ. Even though the changes with ξ in lattice parameters are not very large, it is evident that with increasing ξ, the cell volume V first increases up to $\xi\approx0.7$, then levels off or even slightly decreases for the higher ξ values, except for a step increase near $\xi\approx0.9$. This behavior differs from the general trend of a decreasing V with increasing ξ observed for other $A_2B'B''O_6$ double perovskites.[15] This general trend is found where the valence states of the B' and B'' cations remain the same under ordered and disordered conditions, which we argue is not the case in Sr_2FeMoO_6, where

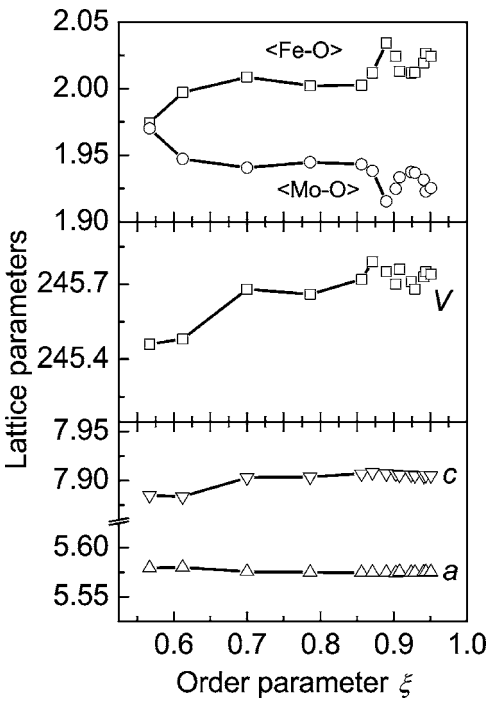

FIG. 2. Dependence of order parameter ξ on lattice parameters a (Å), c (Å), V (Å^3), and average bond length ⟨Fe-O⟩ and ⟨Mo-O⟩ (Å) obtained by Rietveld refinement.

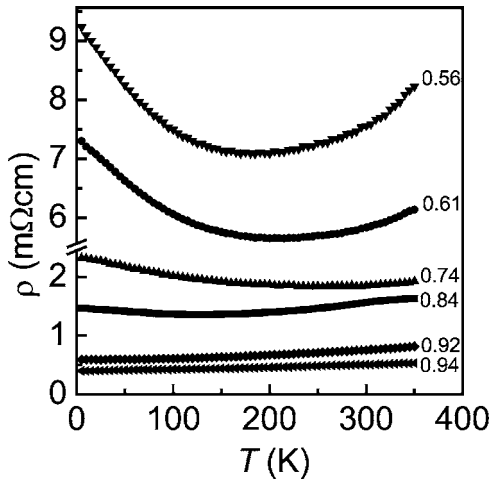

FIG. 3. Temperature dependence of zero-field resistivities for the polycrystalline Sr_2FeMoO_6 samples with different order parameter ξ. All these samples were sintered for 50 h.

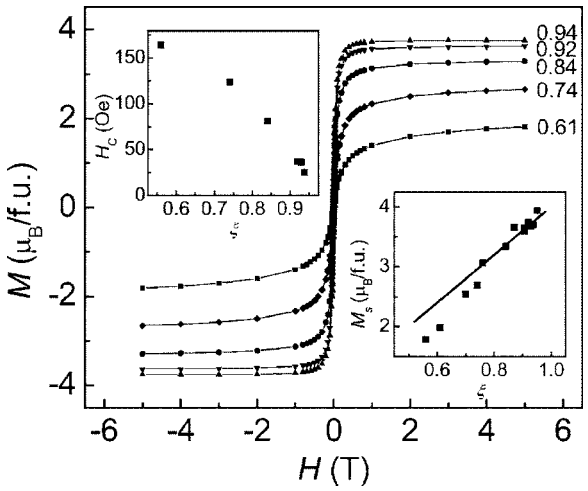

FIG. 4. M-H hysteresis loops at 5 K for Sr_2FeMoO_6 series. Coercivity H_C and saturation magnetization M_s at 5 K as functions of the order parameter ξ are displayed in the left and right inset, respectively. The line in the right inset depicts the theoretical M_s values calculated by $M_s=4\xi\mu_B$/fu.

V increases with ξ. With an ionic model, the average radius of the octahedral-site cations is $r_B=0.63$ Å for an Fe^{III},Mo^V pair (0.645, 0.61 Å) whereas it is $r_B=0.69$ Å for an Fe^{II},Mo^{VI} pair (0.78, 0.59 Å).[16] Therefore V may increase with ξ if order induces a transfer of electrons from Mo-rich clusters to Fe atoms; the trapping of electrons in Mo-rich clusters may occur at grain boundaries or in disordered regions within the bulk. Such an electron transfer appears to occur in the interval $0.56<\xi<0.7$ of Fig. 2. The step in V vs ξ at $\xi\approx0.9$ in Fig. 2 would appear to represent electron transfer by a different mechanism. Such a mechanism would be the transformation of overlapping, polaronic Fe^{III}/Fe^{II} and Mo^{VI}/Mo^V redox couples into an itinerant-electron π^* band. We should therefore expect a transition from polaronic to metallic behavior of the resistance at $\xi\approx0.9$ as well as a decrease in the ⟨Mo-O⟩ bond length and an increase in the ⟨Fe-O⟩ bond length at the sites predominantly occupied by Fe or Mo. In the well-ordered regions that allow π^*-band formation, an oxygen breathing-mode displacement can increase ⟨Fe-O⟩ at one site and decease ⟨Mo-O⟩ at the other so as to induce a greater electron transfer of minority-spin electrons from the Mo to the Fe atoms.

As a further test of this model, we also show in Fig. 2 how the ⟨Fe-O⟩ and ⟨Mo-O⟩ bond lengths change with increasing ξ. As ξ increases from 0.56 to 0.7, the ⟨Fe-O⟩ bonds lengthen and the ⟨Mo-O⟩ bonds shrink as expected for electron transfer from Mo to Fe atoms for $0.56\leqslant\xi\leqslant0.7$, and a step in these changes occurs near $\xi=0.9$. Moreover, as shown in Fig. 3, the resistance changes from polaronic to metallic at $\xi\approx0.9$, whereas at $\xi<0.7$ the resistance is much higher, as expected for a trapping out of charge carriers. In these polycrystalline samples, grain boundaries also affect the transport properties. For example, the polycrystalline Sr_2FeMoO_6 sample initially made by Kobayashi *et al.*[1] exhibited a nonmetallic behavior with a resistivity value of about 0.03 Ω cm at 5 K, whereas a single crystal became metallic with a resistivity of only 2×10^{-4} Ω cm at 5 K.[17] The nanoscaled Sr_2FeMoO_6 polycrystals made by Yuan *et al.*[18] also showed a nonmetallic resistivity of order 10^{-1} Ω cm at 5 K. Niebieskikwiat *et al.*[19] observed an increase by several orders of magnitude in the resistivity of their sample after an oxidation process and claimed that this increase was caused by an oxygen-induced $SrMoO_4$ impurity. If the impurity segregates to the grain boundaries, the resistivity of the polycrystalline sample provides no information on the bulk properties of the grains. However, in our case, all the samples for resistivity measurement in Fig. 3 were sintered for 50 h or even a longer period to lower the influence of grain boundaries, and there was no observable second phase. As can be seen, all the measured samples show resistivities in the $10^{-4}-10^{-3}$ Ω cm range. The resistivity of the $\xi=0.94$ sample is only 4×10^{-4} Ω cm, which is comparable to that of the single crystal.[17] Even for a sample with low ξ, e.g., $\xi=0.56$, the resistivity is less than 10^{-2} Ω cm, much lower than those of the most previous reports on polycrystals. Moreover, the resistivity of our samples varies regularly with the site-order parameter over 20 samples. These observations demonstrate that, in our samples, the transport property is mainly determined by the site ordering. Mössbauer spectroscopy[20] made on well-ordered, paramagnetic samples has shown an effective valence of +2.5 on the Fe atoms as a result of the shared minority-spin electrons in the equilibrium reaction $Fe^{III}+Mo^V=Fe^{II}+Mo^{VI}$. We envisage that with increasing ξ, well-ordered regions are nucleated and grow with increasing T_s. These regions would be separated by a partially disordered boundary that shrinks with increasing ξ to an antiphase boundary across which itinerant electrons can tunnel. A segregation into well-ordered regions with itinerant electrons and partially ordered regions with polaronic conduction would be dictated by the first-order character of the transition from polaronic to itinerant behavior of the electrons.[21]

Figure 4 shows the magnetization M at 5 K as a function of the applied magnetic-field strength H for the Sr_2FeMoO_6 samples. The small remanence and coercivity of the $\xi=0.94$ sample is characteristic of ferromagnetic regions coupled antiferromagnetically across an antiphase boundary.[5]

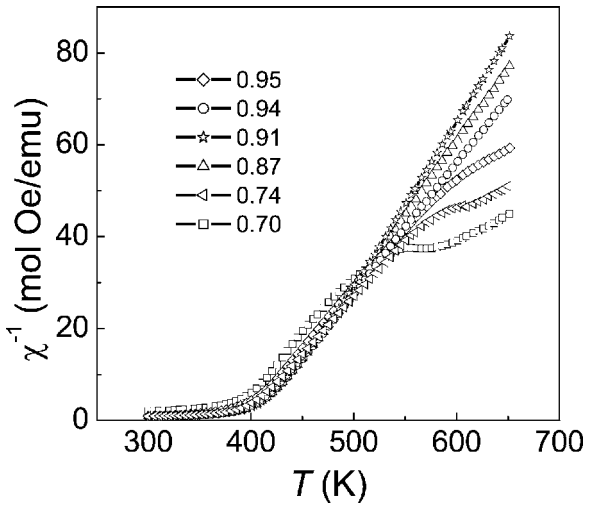

FIG. 5. Reciprocal magnetic susceptibility χ^{-1} taken at 1 T as a function of temperature for Sr_2FeMoO_6 samples with different ξ.

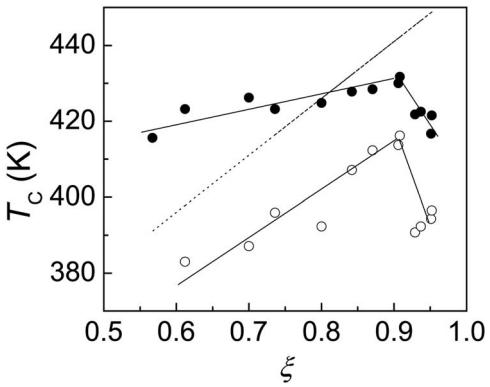

FIG. 6. Dependence of Curie temperature T_C on ξ for Sr_2FeMoO_6 samples. Solid circles represent the values obtained from $M(T)$ data; open circles give the Weiss temperature determined by the Curie-Weiss law. The dotted line shows the ξ dependence of the predicted T_C values according to the Monte Carlo simulation in Ref. 10.

The saturation magnetization M_s was attained from the extrapolation of M vs $1/H$ to $1/H=0$. M_s exhibits a linear increase with ξ in the interval of $0.7 \leqslant \xi \leqslant 0.95$; see the inset of Fig. 4. An $M_s=3.96\mu_B$/fu for the $\xi=0.95$ sample approaches the ideal predicted value of $4\mu_B$/fu. In the interval $0.7 \leqslant \xi \leqslant 0.95$, but not for $\xi<0.7$, the ξ dependence of M_s is in accord with the theoretical prediction $M_s=4\xi\mu_B$/fu for the case that no minority-spin electrons become spin paired in molecular orbitals of Mo-rich traps. This observation is consistent with a trapping of minority-spin electrons in Mo-rich clusters that is restricted to $\xi<0.7$, which is in accord with our deduction from changes in V with ξ in Fig. 2.

$M(T)$ curves taken at $H=1$ T show a well-defined magnetic-ordering temperature for samples with $\xi \geqslant 0.7$. Reciprocal magnetic susceptibilities $\chi^{-1}(T)$ taken at 1 T are shown in Fig. 5, and the T_C and Weiss constants θ are shown in Fig. 6. As has been shown in a previous publication,[5] the $\chi^{-1}(T)$ curves depend strongly on the measuring field; θ increases with H from $\theta<T_C$ as in a ferrimagnet to $\theta \geqslant T_C$ as in a ferromagnet. Where a $\theta<T_C$ is found, the $\chi^{-1}(T)$ curves bend above T_C as in a ferrimagnet and approach a straight line for $\theta \geqslant T_C$. This trend is evident in Figs. 5 and 6, which makes the interpretation of μ_{eff} treacherous. To what extent this behavior reflects antiferromagnetic coupling across antiphase boundaries on the one hand and, on the other hand, a shift in the minority-spin electrons between Mo and Fe sites in the applied magnetic field is undetermined. More meaningful, therefore, are the T_C values of Fig. 6. We determined the T_C values by a linear extrapolation of the tangent at the inflection point of the $M(T)$ curves taken at $H=1$ T. The T_C values vary little with the strength of H. The observation of a maximum T_C at $\xi \approx 0.9$, where the slope of $\rho(T)$ changes from polaronic to metallic in Fig. 3, is noteworthy. These data imply that the maximum T_C occurs where the conductive minority-spin electrons have a phonon-assisted mobility ($\tau_h \approx \omega_0^{-1}$, where ω_0^{-1} is the period of optical-mode vibrations that trap the electrons as small polarons). As the π^* band broadens with increasing ξ, the density of the one-electron state at the Fermi energy decreases and the coupling of the localized majority-spin electrons by the minority-spin electrons can be expected to decrease.

IV. CONCLUSIONS

Interpretation of the effect of site disorder on the magnetic properties of the double perovskite Sr_2FeMoO_6 is made complex by an equilibrium reaction $Fe^{III}+Mo^{V}=Fe^{II}+Mo^{VI}$ that is shifted to the left by trapping out of charge carriers in Mo-rich clusters and by a shifting to the right in well-ordered regions, where a periodic potential transforms polaronic minority-spin electrons into itinerant electrons. Moreover, the presence of antiphase boundaries in well ordered samples gives rise to Curie-Weiss behavior that depends strongly on the applied magnetic field. In addition, the transition from polaronic to itinerant electronic behavior is normally first order, which should lead to a segregation of well-ordered and partially ordered regions. Consequently, theoretical models of magnetic behavior that are based on a homogeneous distribution of antisite disorder and fixed numbers of minority-spin electrons on the Fe and Mo atoms need to be reconsidered. The model of Frontera and Fontcuberta[22] may be applicable in the region $0.7<\xi<0.9$, but an adjustment to the ferromagnetic exchange parameter would seem to be necessary for $\xi \geqslant 0.9$ where our data indicate an itinerant-electron phase is introduced.

ACKNOWLEDGMENTS

The present work was supported by Grants-in-Aid for Scientific Research (No. 15206002 and No. 15206071) from the Japan Society for the Promotion of Science. Y. H. Huang acknowledges the Japan Society for the Promotion of Science for awarding him the Foreigner Postdoctoral Fellowship (ID P02315). J.B.Goodenough thanks the Robert A. Welch Foundation, Houston, Texas, for financial support.

*Electronic address: huangyh@mail.utexas.edu

[1] K.-I. Kobayashi, T. Kimura, H. Sawada, K. Terakura, and Y. Tokura, Nature (London) **395**, 677 (1998).
[2] J. B. Goodenough, Mater. Res. Bull. **6**, 967 (1971).
[3] T. Saitoh, M. Nakatake, A. Kakizaki, H. Nakajima, O. Morimoto, Sh. Xu, Y. Moritomo, N. Hamada, and Y. Aiura, Phys. Rev. B **66**, 035112 (2002).
[4] J.-S. Kang, J. H. Kim, A. Sekiyama, S. Kasai, S. Suga, S. W. Han, K. H. Kim, T. Muro, Y. Saitoh, C. Hwang, C. G. Olson, B. J. Park, B. W. Lee, J. H. Shim, J. H. Park, and B. I. Min, Phys. Rev. B **66**, 113105 (2002).
[5] J. B. Goodenough and R. I. Dass, Int. J. Inorg. Mater. **2**, 3 (2000).
[6] B. Martínez, J. Navarro, Ll. Balcells, and J. Fontcuberta, J. Phys.: Condens. Matter **12**, 10515 (2000); M. Tovar, M. T. Causa, A. Butera, J. Navarro, B. Martínez, J. Fontcuberta, and M. C. G. Passeggi, Phys. Rev. B **66**, 024409(R) (2002).
[7] D. Sánchez, M. García-Hernández, J. L. Martínez, J. A. Alonso, M. J. Martínez-Lope, M. T. Casais, and A. Mellergård, J. Magn. Magn. Mater. **242-245**, 729 (2002).
[8] D. Niebieskikwiat, R. D. Sánchez, A. Caneiro, L. Morales, M. Vásquez-Mansilla, F. Rivadulla, and L. E. Hueso, Phys. Rev. B **62**, 3340 (2000).
[9] Y. H. Huang, J. Lindén, H. Yamauchi, and M. Karppinen, Chem. Mater. **16**, 4337 (2004).
[10] A. S. Ogale, S. B. Ogale, R. Ramesh, and T. Venkatesan, Appl. Phys. Lett. **75**, 537 (1999).
[11] T. Yamamoto, J. Liimatainen, J. Lindén, M. Karppinen, and H. Yamauchi, J. Mater. Chem. **10**, 2342 (2000); T. Shimada, J. Nakamura, T. Motohashi, H. Yamauchi, and M. Karppinen, Chem. Mater. **15**, 4494 (2003).
[12] F. Izumi and T. Ikeda, Mater. Sci. Forum **321**, 198 (2000).
[13] O. Chmaissem, R. Kruk, B. Dabrowski, D. E. Brown, X. Xiong, S. Kolesnik, J. D. Jorgensen, and C. W. Kimball, Phys. Rev. B **62**, 14197 (2000).
[14] P. M. Woodward, Acta Crystallogr., Sect. B: Struct. Sci. **53**, 32 (1997).
[15] P. Woodward, R.-D. Hoffmann, and A. W. Sleight, J. Mater. Res. **9**, 2118 (1994).
[16] R. D. Shannon, Acta Crystallogr., Sect. A: Cryst. Phys., Diffr., Theor. Gen. Crystallogr. **32**, 751 (1976).
[17] Y. Tomioka, T. Okuda, Y. Okimoto, R. Kumai, K.-I. Kobayashi, and Y. Tokura, Phys. Rev. B **61**, 422 (2000).
[18] C. L. Yuan, S. G. Wang, W. H. Song, T. Yu, J. M. Dai, S. L. Ye, and Y. P. Sun, Appl. Phys. Lett. **75**, 3853 (1999).
[19] D. Niebieskikwiat, A. Caneiro, R. D. Sánchez, and J. Fontcuberta, Phys. Rev. B **64**, 180406(R) (2001).
[20] J. Lindén, T. Yamamoto, M. Karppinen, H. Yamauchi, and T. Pietari, Appl. Phys. Lett. **76**, 2925 (2000).
[21] J. B. Goodenough, Struct. Bonding (Berlin) **98**, 1 (2001).
[22] C. Frontera and J. Fontcuberta, Phys. Rev. B **69**, 014406 (2004).